第 34 卷第 5 期
2018 年 5 月

无 机 化 学 学 报
CHINESE JOURNAL OF INORGANIC CHEMISTRY

Vol.34 No.5
942-950

一种家蚕茧衍生具有蜂窝状结构的钴–锰共掺杂碳材料双功能电解水催化剂

张 明*,[1] 李 涛[1] 王 娟[1] 潘 逸[1] 马仕杰[1] 朱 罕[2] 杜明亮[2]

([1]浙江理工大学材料与纺织学院,先进纺织材料与制备技术教育部重点实验室,杭州 310018)

([2]江南大学化学与材料工程学院,合成与生物胶体教育部重点实验室,无锡 214122)

摘要:通过一步碳化石墨化过程,由家蚕茧制得了一种具有蜂窝状结构的氮钴锰共掺杂碳材料。该材料具有蜂窝状结构和高比表面积,同时由于暴露的钴–锰活性位点以及富含的吡啶氮和石墨氮,3%钴–锰/蚕茧的碳材料(3%Co-Mn/SCC)显示了高析氢反应活性,其初始电位和 10 mA·cm^{-2} 过电位分别只有 121 和 155 mV,Tafel 斜率为 130 mV·dec^{-1},并且在酸性条件下具有很好的稳定性。与此同时,2%Co-Mn/SCC 在碱性条件下表现出优异的析氧反应催化性能,具有较低的初始电位,Tafel 斜率为 143 mV·dec^{-1}。

关键词:碳材料;家蚕茧;双功能催化;电解水

中图分类号:TQ116.2^{+}1;O614.7^{+}1;O614.81^{+}2 **文献标识码**:A **文章编号**:1001-4861(2018)05-0942-09

DOI:10.11862/CJIC.2018.122

Honeycomb-like Structured and Co-Mn Incorporated Carbon Materials Derived from *Bombyx mori* Cocoons Act as a Bifunctional Catalyst for Water Splitting

ZHANG Ming*,[1] LI Tao[1] WANG Juan[1] PAN Yi[1] MA Shi-Jie[1] ZHU Han[1,2] DU Ming-Liang[1,2]

([1]*Key Laboratory of Advanced Textile Materials and Manufacturing Technology of the Ministry of Education, College of Materials and Textiles, Zhejiang Sci-Tech University, Hangzhou* 310018, *China*)

([2]*Key Laboratory of Synthetic and Biological Colloids, Ministry of Education, School of Chemical and Material Engineering, Jiangnan University, Wuxi, Jiangsu* 214122, *China*)

Abstract: Porous and graphene-type honeycomb-like structured N-doped and Co-Mn incorporated carbon materials derived from *Bombyx mori* silk cocoons were synthesized via one-step thermal carbonization and graphitization process. Due to the high specific surface area of honeycomb-like structure, the exposed Co-Mn active sites and the pyridine-N and graphitic-N, the prepared 3% Co-Mn/silk cocoon carbon materials (3% Co-Mn/SCC) exhibits good hydrogen evolution reaction (HER) performance with a low onset potential of 121 mV, a low overpotential of 155 mV at 10 mA·cm^{-2} and a Tafel slope of 130 mV·dec^{-1} as well as a long-term stability in acidic electrolyte. Meanwhile, the 2%Co-Mn/SCC also shows great oxygen evolution reaction (OER) performance in 1 mol·L^{-1} KOH with the lowest onset potential 1.5 mV and a Tafel slope of 143 mV·dec^{-1}. This result demonstrates that *M*Co-Mn/SCC (*M* is the mass fraction of Co and Mn) possess both HER and OER catalytic activity and can act as a bifunctional catalyst for water electrolysis.

Keywords: carbon materials; *Bombyx mori* silk cocoons; bifunctional catalyst; water splitting

收稿日期:2017-11-13。收修改稿日期:2018-03-17。

国家自然科学基金(No.51573166)和浙江省自然科学基金(No.LQ16E020005)资助项目。

*通信联系人。E-mail:zhangming@zstu.edu.cn

0 Introduction

In the next few decades, fossil-fuel crisis, demand for energy resources and environmental pollution continue to worsen, the clean, environmental friendly and renewable energy sources would play a supreme important role. Hydrogen fuel, as one of the most ideal clean energy, has recently aroused considerable attention because its high heating value and pollution-free[1-3]. Currently, electrocatalytic water splitting has been recognized as one of the most promising method for producing hydrogen. Nevertheless, the overall water splitting efficiency is greatly influenced by the hydrogen evolution reaction (HER) and oxygen evolution reaction (OER) as a result of multistep proton-coupled electron transfer process[4-6]. Therefore, much effort has been made to accelerate the HER and OER reaction kinetics and dropping the requirement of overpotential. To the best of our knowledge, Pt-based electrocatalysts are known as the most effective HER catalysts[7] and Ru or Ir-based electrocatalysts exhibit the most effective OER catalytic activity[8-11]. However, the widespread application has been significantly hindered by the limited reserves and high costs. Hence, one of the main challenges in renewable energy research has been developing sustainable, cost-effective and earth-abundant electrocatalysts.

In a variety of electrode materials, graphene, which has high specific surface area of all carbon materials is extensively used in the fields of electrocatalytic water splitting because of its high specific surface area, superb electrical conductivity, high mechanical strength and low cost[12-15]. Furthermore, N-doped graphene materials demonstrate higher catalytic activity in electrocatalysts[16-18]. Recent studies suggest that among these specimens, pyridinic and graphitic nitrogen both serve as active site which play an important role in the catalytic process[19-21]. Nevertheless, N-doped graphene materials almost are used as monofunctional catalysts, and enormous potential of bifunctional or multifunctional catalysts have not been widely investigated so far. In addition, at present, preparations of N-doped graphene materials by hydrothermal reaction and thermolysis with extra N resource into their precursor are inefficient. Thanks to the high N element content, many biomass[22-24], for example silk, are expected to be ideal precursors for porous N-doped graphene materials, which usually exhibit impressive catalytic performance for HER and OER[25].

As previous reported, some carbon materials incorporated with metals have been applied to electrocatalysis and demonstrated improved electrocatalytic performance[26-28]. Recently, transition metal nanoparticles (Co, Mn, Ni, Cu, *etc*.) coated with carbon layers have been found to be one of most effective electrocatalysts[29-33]. Theoretically, the incorporated metal nanoparticles increase the active site greatly; moreover, certain multiple-metal co-incorporated systems can exhibit synergistic effects in transition metal clusters and further improve the catalytic activity, and the carbon layer on the surface of the metal can protect the metal from coming into being metallic oxides[34]. However, the growth of transition metal in carbon materials derived from biomass and its electrochemical properties have not been thoroughly studied.

In this study, we develop a simple approach to synthesize porous and graphene-like carbon materials from *Bombyx mori* silk cocoons by an effective thermal carbonization strategy. *Bombyx mori* possesses an oriented β-sheet crystal structure (high-ordered silk II structure) with a lamellar-like layer and highly porous nonwoven structure. As reported, *Bombyx mori* silk cocoons are composed of sericin and fibroin. After the thermal carbonization process, the sericin are eliminated[24]. Proteins that make up the silk fibroin consist of 18 types of amino acid. In addition, recent reports have demonstrated that activated by KCl solution, the silk nanostructure shows excellent HER performance.

In this work, we prepared honeycomb-like structured Co-Mn incorporated N-doped graphene materials by a facile thermal carbonization process of an abundant biomass, *Bombyx mori* silk cocoons, as catalyst for electrolysis of water, which demonstrate

amazing HER and OER performance. These encouraging results may offer a facile and effective method for the preparation of bifunctional catalysts derived from natural sustainable biomass.

1 Experimental

1.1 Synthesis and method

Bombyx mori silk cocoons were first stripped with the outermost and the innermost and then washed by DI water three times to remove impurities. The cocoons were torned into small pieces. Secondly, cobalt nitrate and manganese acetate were dissolved into DMF with different proportion solution (the total mass fraction of Co and Mn is 0.5%, 2%, 3% and 5%, w_{Co}:w_{Mn}=1:1). The cocoons were immersed into solution for 24 hours at room temperature and dried in a vacuum oven at 40 ℃. The cocoons were placed into a ceramic boat, carbonized at 800 ℃ under Ar and NH_3 atmosphere (Ar: 150 mL·min^{-1}, NH_3: 10 mL·min^{-1}) for 4 h with a heating rate of 5 ℃·min^{-1}, and cooled down to room temperature naturally. The obtained products were washed with 0.5 mol·L^{-1} H_2SO_4 aqueous solution and dried at 60 ℃for 24 h in a vacuum oven, which were denoted as *M*Co-Mn/SCC (*M* is the total mass fraction of Co and Mn).

1.2 Characterizations

Field-emission scanning electron microscopic (FE-SEM, JEOL, Japan) measurements at an acceleration voltage of 3 kV were used to characterize the morphology of all the samples. Transmission electron microscopic (TEM) measurements at an acceleration voltage of 200 kV were carried out by a JEOL JSM-2100 microscope. Powder X-ray diffraction (XRD) patterns of the samples were recorded on a SIEMENS Diffraktometer equipped with Cu *Kα* radiation (λ= 0.154 06 nm) at 35 kV in the 2θ range of 10°~80°. X-ray photoelectron spectroscopic (XPS) measurements were obtained using a Kratos Axis Ultra DLD.

1.3 Electrochemistry

The HER and OER electrochemical perform measurements were evaluated with a typical three-electrode system using an electrochemical workstation (CHI 660D) in 0.5 mol·L^{-1} H_2SO_4 and 1 mol·L^{-1} KOH electrolytes, respectively. The samples were cut into 1 cm×1 cm and directly used as the working electrode. A platinum gauze and a saturated calomel electrode were used as counter electrode and reference electrode. In all measurements, the potentials were reported versus a reversible hydrogen electrode (RHE). Linear sweep voltammetry (LSV) with a scan rate of 2 mV·s^{-1} was recorded in 0.5 mol·L^{-1} H_2SO_4 and 1 mol·L^{-1} KOH, respectively. Cyclic voltammetry (CV) was obtained to evaluate the long-term catalysis stability at a sweep rate of 50 mV·s^{-1}.

2 Results and discussion

To further improve the electrochemical performance, we incorporated Co-Mn with different fraction. Compared with pure silk fibroin (Fig.S1), which demonstrates a small amount of pores on surface, the samples treated with the cobalt nitrate and manganese acetate and carbonization at 800 ℃ under Ar/NH_3 atmosphere have a rough surface. The content of Co-Mn will obviously influence the morphology. At the same time, the metal particles are evenly dispersed on the surface of silk fibers. Fig.1a shows the low-magnification SEM image of the as-obtained 0.5%Co-Mn/SCC, which possesses a morphology with metal particles covering the surface but without any apparent pores. With the metal concentration increased to 2% (Fig.1b), large amounts of pores are dispersed inhomogeneously on its surface. When the content of Co-Mn was further increased to 3% (Fig.1c), the pores with the size range of 50~150 nm are distributed uniformly on the surface of carbonized silk cocoons, forming honeycomb-like network structure. This continuous honeycomb-like morphology has been well recognized as the ideal structure for water electrolysis because of shortening the ion diffusion paths during the charge/discharge process, at the same time honeycomb-like pores can act as ions storage buffer between the electrolyte solution and electrode material. In addition, metal nanoparticles can be observed distributed at the cross-link sections which play an important role of exposing more active sites to further improve the electrochemical performance. The

sample of 5% Co-Mn/SCC is shown in Fig.1d, it can be observed that the original morphology collapses from the honeycomb-like network into a compact concave appearance, which is mainly ascribed to the excessive concentration of Co and Mn ions. The honeycomb-like network was further confirmed by TEM, as shown in in Fig.S2, nearly no porous structure was observed in 0.5% Co-Mn/SCC and 5% Co-Mn/SCC, however, 2% Co-Mn/SCC and 3% Co-Mn/SCC form the network structure consisting of macropores with diameter of approximately 50 nm corresponding to the Fig.1c, and obviously, all samples exist graphene sheets and metal nanoparticles. It is noteworthy that agglomeration occurs for the 5% Co-Mn/SCC metal and the porous structure begin collapse as shown in Fig.S2d. Through the Fig.1(e,f), we noticed that the nanoparticles are covered by graphitic carbon layers and the interlayer distance of the surrounded carbon is 0.37 nm, which are assigns to the (002) plane of carbon. To further confirm the porous characteristics of the resultant honeycomb-like carbon materials, nitrogen adsorption-desorption measurements were conducted. The N_2 adsorption-desorption isotherms obtained by the quenched solid density functional theory (QSDFT) method for the as-prepared samples are shown in Fig.S3. It can be found that all the samples exhibit combined Ⅰ and Ⅳ type adsorption-desorption isotherms with N_2 adsorption at relatively low pressure and slightly steep adsorption in the relative pressure range of 0.8~1.0 (Fig.S3), indicating the coexistence of the micropores, mesopores and/or macropores in the materials. The pure silk fibroin only exhibits a BET surface area of 10 $m^2 \cdot g^{-1}$. With the incorporation of Co-Mn, the surface area of the 0.5% Co-Mn/SCC, 2% Co-Mn/SCC and 3% Co-Mn/SCC increases to 148, 151 and 315 $m^2 \cdot g^{-1}$, respectively. However, 5% Co-Mn/SCC exhibits the surface area of 105 $m^2 \cdot g^{-1}$, indicating the evolution of pore architectures of the carbon materials derived from *Bombyx mori* cocoons.

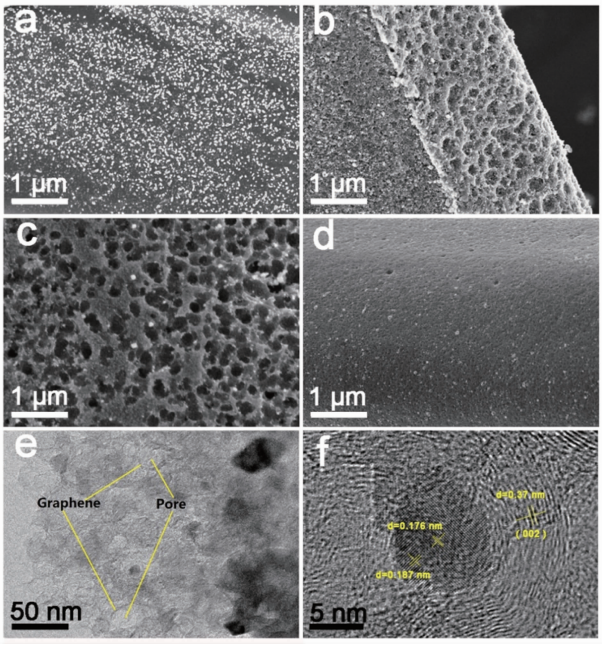

(a) 0.5%Co-Mn/SCC, (b) 2%Co-Mn/SCC, (c) 3%Co-Mn/SCC, (d) 5%Co-Mn/SCC

Fig.1　FE-SEM images of *M*Co-Mn/SCC (a~d) and TEM images of 3%Co-Mn/SCC (e, f)

The sample has been thoroughly investigated by STEM-EDS mapping (Fig.2(a,b)). The results of elemental distribution indicate uniform distribution of C, N and O elements and with the line-scan EDX spectra (Fig.2c), we may conclude that part of the incorporated Co-Mn has already converted into metal-oxide and after washed with 0.5 $mol \cdot L^{-1}$ H_2SO_4 aqueous solution, some have been removed, the mass fraction of Co-Mn is different from the original. To further investigate the microstructure of the carbonized silk cocoon and the crystalline structure of the Co-Mn oxide, the XRD patterns of the samples are presented in Fig.2d. All samples exhibit the same XRD pattern of Co_3Mn_7 (PDF No.18-0407) (it is also confirmed by Fig.1f, d=0.176 and d=0.187 nm corresponding to the Co_3Mn_7) and (Co,Mn) $(Mn,Co)_2O_4$ (PDF No.18-0409). Interestingly, all samples, excepting for 5% Co-Mn/SCC, exhibit a broad diffraction peak at around 24° corresponding to the (002) plane of graphite, demonstrating the amorphous nature and low graphitization degree. When the Co-Mn concentration increased from 0.5% to 3%, the peaks get stronger and sharper, indicating the improvement of crystallinity. However, the diffraction peak exhibit relatively lower intensity, corresponding to the lower crystallinity resulted from the metal agglomeration and over-doping of elements

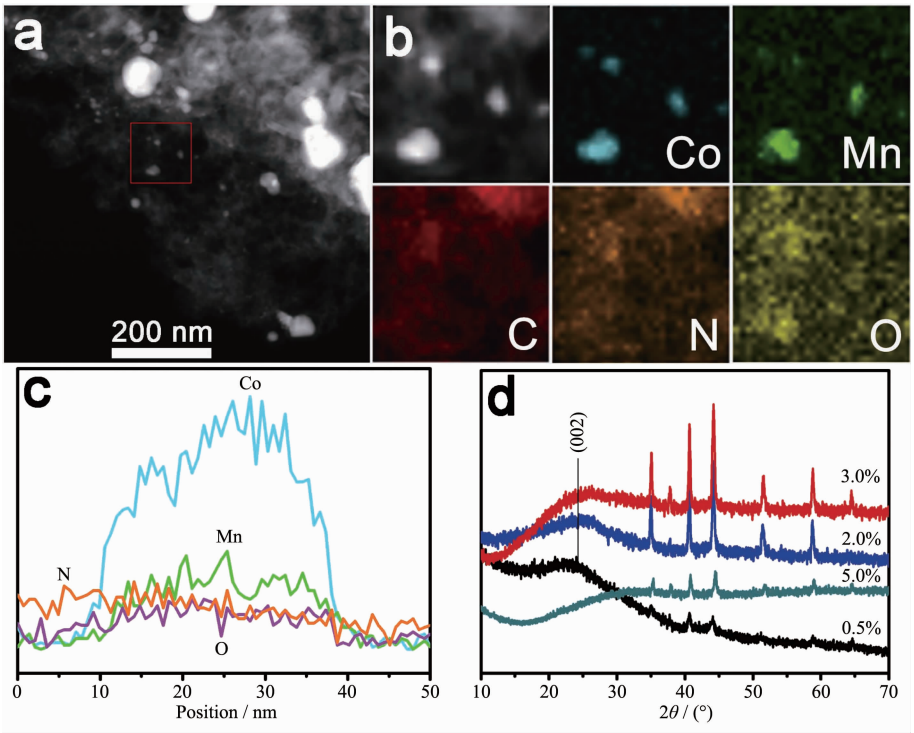

Fig.2 (a) HAADF-STEM image, (b) STEM-EDS mapping images and (c) line-scan EDX spectra of 3%Co-Mn/SCC; (d) XRD patterns of *M*Co-Mn/SCC

with excessive Co-Mn.

X-ray photoelectron spectroscopy (XPS) measurements were utilized to further investigate the chemical composition and surface chemistry of 3%Co-Mn/SCC. The XPS survey spectrum of the 3%Co-Mn/SCC presented in Fig.S4 displays the corresponding peaks of C, N, O, Co and Mn with no further evidence of any impurities. The high-resolution C1*s* spectrum could be fitted to three peaks (Fig.3a) located at approximately 284.7, 285.1 and 285.9 eV, which corresponds to the graphite C bonds, the C-N and C-H bonds resulting from displacement of the N atoms and the defects of the N-doped carbon fibers. Owing to nitrogen existence of N-doped silk carbon fibers (2.5% (*w*/*w*) as indicated in Fig.S5), the chemical states of nitrogen were further investigated by obtaining high-resolution N1*s* peaks (Fig.3b). Deconvolution of the high-resolution scan of the N1*s* electrons yielded three peaks at the binding energies of 401.6, 400.3, and 398.6 eV, which are assigned to the graphitic nitrogen (N-Q), pyrrole-like nitrogen (N-5), and pyridinic -like nitrogen (N-6), respectively. Compared with N-5, N-Q and N-6 show more intense peaks. In other words, the active nitrogen species (pyridinic-like nitrogen and graphitic nitrogen)[15] occupy the main part of nitrogen element. The different valence state of the Co species and Mn species of were also detected by Co2*p* and Mn2*p* spectrum (Fig.3(c,d)). It demonstrates that the Co species were mainly in the oxidation state of approximately +3.0 and Mn species correspond to metal-oxide.

The electrocatalytic activities for HER and OER were then using a typical three-electrode system with electrochemical measurements in 0.5 mol·L^{-1} H_2SO_4 and 1 mol·L^{-1} KOH, respectively at room temperature. The overpotential at 10 mA·cm^{-2} versus a reversible hydrogen electrode (RHE) is used to evaluate the HER performance. Fig.4a shows the linear sweep voltammetric (LSV) of 0.5%Co-Mn/SCC, 2.0%Co-Mn/SCC, 3.0%Co-Mn/SCC and 5.0% Co-Mn/SCC for HER. Obviously, the 3.0% Co-Mn/SCC reveal the best HER activity with a lower onset potential of 121 mV and an overpotential of 155 mV among four samples. According to Fig.S6, 3.0%Co-Mn/SCC shows the best HER activity compared with 3.0% Co/SCC, 3.0% Mn/SCC and SCC. It implies that, through the incorporation of

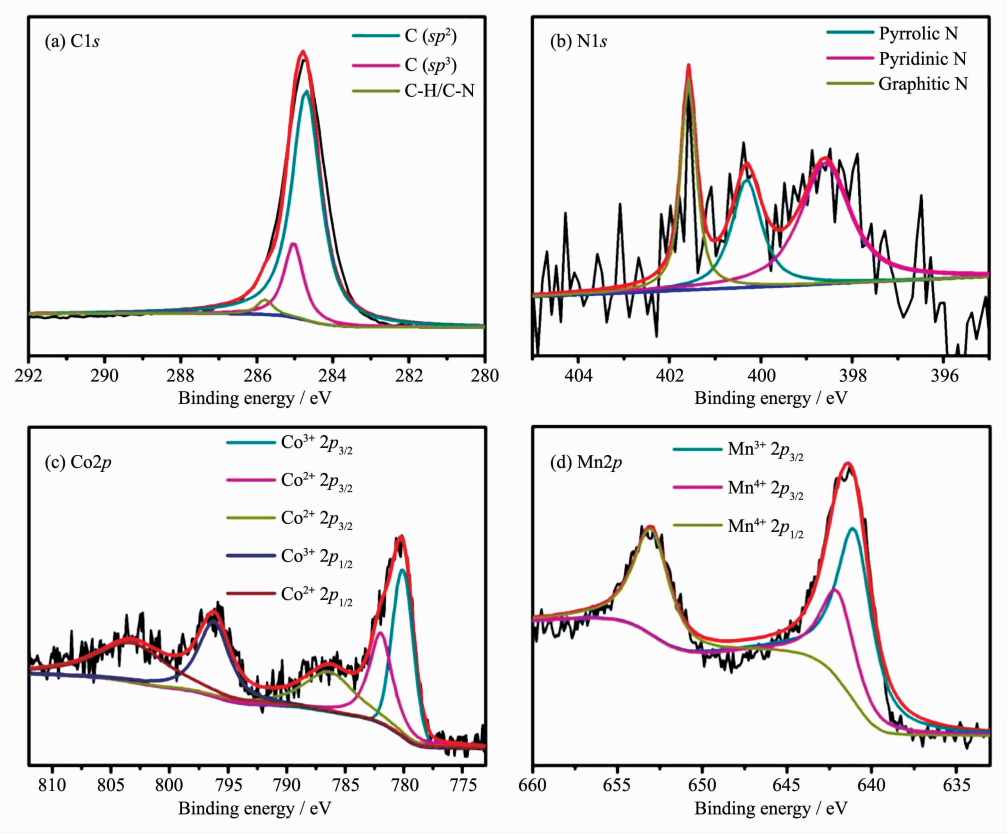

Fig.3　XPS spectra of the 3%Co-Mn/SCC

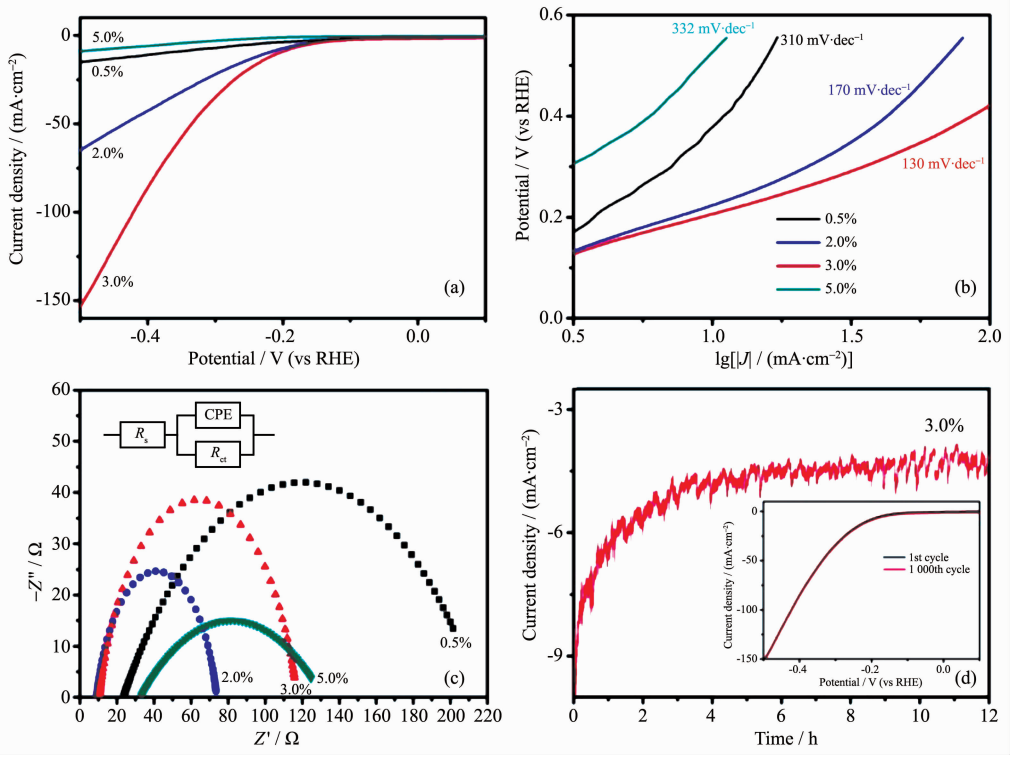

(a, b) in 0.5 mol·L^{-1} H_2SO_4 with a scan rate of 2 mV·s^{-1}; Inset in (d) is polarization curves of 3.0%Co-Mn/SCC

Fig.4　(a) Polarization curves, (b) corresponding Tafel slopes and (c) Nyquist plots performed at −0.25 V vs RHE of *M*Co-Mn/SCC; (d) Time-dependent current density of the 3.0%Co-Mn/SCC at a constant voltage of −0.2 V vs RHE

Co and Mn, more active sites were exposed and with the formation of Co_3Mn_7, the HER performance is further improved. What's more, the results imply that the HER performance was improved with the increase of Co-Mn concentration. However, the 5.0% Co-Mn/SCC catalyst exhibits poor activity, which is ascribed to the collapse of honeycomb-like network. The results suggest that the samples exhibit high electrocatalytic activity with only a small content of Co-Mn.

To further investigate the catalytic kinetics of HER process, the Tafel plots are calculated by the Tafel equation ($\eta=a+b\lg|J|$, where J is the current density, a and b are constant; and η is the onset potential) to evaluate the rate determining step (RDS) (Fig.4b). Tafel slopes of 0.5% Co-Mn/SCC, 2.0% Co-Mn/SCC, 3.0% Co-Mn/SCC and 5.0% Co-Mn/SCC are 310, 170, 130 and 332 mV·dec^{-1} respectively. The 3.0%Co-Mn/SCC catalyst possesses the minimum Tafel slope, implying a drastic increase of HER currents with increasing electrode potential and hence better HER performance. Electrochemical impedance spectroscopy (EIS) is another index to evaluate the interface reactions and electrode kinetics of catalysts. As shown in Fig.4c, where R_s is the solution resistance and CPE is the parallel connection, the Nyquist plots of the 2.0% Co-Mn/SCC and 3.0% Co-Mn/SCC have smaller resistance and charge transfer resistance (R_{ct}) value of 73 and 117 Ω, respectively, which denote high conductivity and fast electron transmission. In addition, after 12 hours continuous electrocatalytic operations, the current density of 3.0% Co-Mn/SCC show almost negligible drop and after long-term cycling, the current density retention rate is 80%, the bubble accumulate on the catalyst surface at the first two hours, which is not conducive to the electron transport process, resulting in the current density attenuation (Fig.4d). After that, the number of bubbles is stable, and the current density is further stabilized. The polarization curves of 3.0%Co-Mn/SCC also shows a negligible decay in cathodic currents after 1 000 cycles, which demonstrates the superior cycle stability (inset in Fig.4d).

Additionally, we also explore the OER performance of M-Co-Mn/SCC (Fig.5). LSV measurements (Fig.5a) reveal that 2.0% Co-Mn/SCC exhibits the lowest onset potential of 1.5 V, which is very close to that of a high-surface-area commercial IrO_2 catalyst (≈1.47 V) with respect to a reversible hydrogen electrode (RHE) much lower than that of Pt/C catalysts (1.76 V)[29]. Compared with 5.0%Co-Mn/SCC and 3.0% Co-Mn/SCC, 2%Co-Mn/SCC exhibits the smaller Tafel slope of 143 mV·dec^{-1} (Fig.5b), which is lower than that of Pt/C (170 mV·dec^{-1}), indicating its rapid OER reaction kinetics.

In the present investigations, the change of ion concentration leads to the evolution of the morphology and structure of the Co-Mn/SCC, resulting in the oxygen-deficient structures and enhanced OER and HER activity. The material exhibit several advantages: (1) Catalysts are prepared by a carbon resource derived from silk cocoons, which are an environmental friendly and renewable biomass, without any extra N

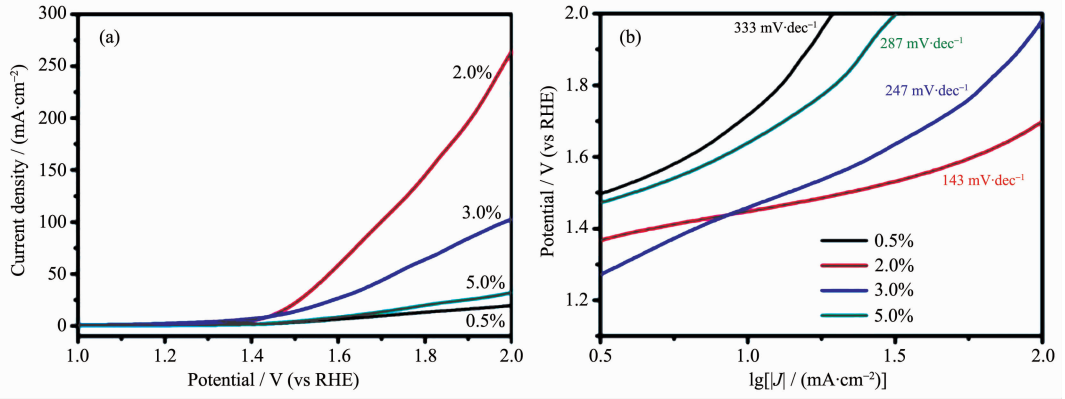

Fig.5 (a) Polarization curves and (b) corresponding Tafel slopes of *M*Co-Mn/SCC obtained in 1 mol·L^{-1} KOH with a scan rate of 2 mV·s^{-1}

resource into precursor; (2) The honeycomb-like structured graphene materials show a hierarchical porous structure and a large specific surface area, and through the co-incorporation of Co and Mn, more active sites were exposed; (3) The honeycomb-like structured graphene materials were synthesized through a facile process and no templates or reagents were utilized; (4) The honeycomb-like structured graphene materials function as a bifunctional catalyst for electrocatalytic water splitting with high catalytic activity and outstanding stability as well as durability.

3 Conclusions

Porous and graphene-type honeycomb-like structured N-doped and Co-Mn incorporated carbon materials used as a bifunctional catalyst for electrocatalytic water splitting were designed and synthesized. Because of the high specific surface, the exposed Co-Mn active sites and the rich pyridine-N and graphitic-N, M-Co-Mn/SCC shows good HER and OER catalytic activity. In particular, 3% Co-Mn/SCC exhibits high HER performance with a low onset potential of 121 mV, a low overpotential of 155 mV at 10 $mA \cdot cm^{-2}$ and a Tafel slope of 130 $mV \cdot dec^{-1}$ as well as long-term stability in acidic electrolyte, and the 2% Co-Mn/SCC shows great oxygen evolution reaction (OER) performance in 1 $mol \cdot L^{-1}$ KOH with the lowest onset potential 1.5 mV and a Tafel slope of 143 $mV \cdot dec^{-1}$. These encouraging results may offer a facile and effective method for the preparation of bifunctional catalyst catalysts derived from naturally sustainable biomass.

Supporting information is available at http://www.wjhxxb.cn

References:

[1] Li J S, Wang Y, Liu C H, et al. *Nat. Commun.*, **2016**,**7**: 11204(8 Pages)

[2] Ray C, Dutta S, Negishi Y, et al. *Chem. Commun.*, **2016**,**52** (36):6095-6098

[3] Subbaraman R, Tripkovic D, Strmcnik D, et al. *Science*, **2011**,**334**(6060):1256-1260

[4] Youngblood W J, Lee S H A, Maeda K, et al. *Acc. Chem. Res.*, **2009**,**42**(12):1966-1973

[5] Kanan M W, Nocera D G. *Science*, **2008**,**321**(5892):1072-1075

[6] Zhu H, Yu D N, Zhang S G, et al. *Small*, **2017**,**13**:1700468

[7] Lv H F, Xi Z, Chen Z Z, et al. *J. Am. Chem. Soc.*, **2015**,**137** (18):5859-5862

[8] Jackson A, Viswanathan V, Forman A J, et al. *ChemElectro Chem*, **2014**,**1**(1):67-71

[9] Cid R E, de la Fuente J L G, Rojas S, et al. *ChemCatChem*, **2013**,**5**(12):3680-3689

[10]Pei J J, Mao J J, Liang X, et al. *Chem. Commun.*, **2016**,**52** (19):3793-3796

[11]Thomassen M S, Mokkelbost T, Sheridan E, et al. *ECS Meeting*: *Vol.*35. Zaghib K, Julienet C, Chiu W, et al. Ed., New Jersey: Electrochemical Society, **2011**:271-279

[12]Bridewell V L, Kareacki C J, Kamat P V. *ACS Sens.*, **2016**, **1**(10):1203-1207

[13]Cui H J, Yu H M, Zheng J F, et al. *Nanoscale*, **2016**,**8**(5): 2795-2803

[14]Chanda D, Hnat J, Dobrota A S, et al. *Phys. Chem. Chem. Phys.*, **2015**,**17**(40):26864-26874

[15]Yoo E, Okata T, Akita T, et al. *Nano Lett.*, **2009**,**9**(6):2255-2267

[16]Yang S B, Feng X L, Wang X C, et al. *Angew. Chem. Int. Ed.*, **2011**,**50**(23):5339-5343

[17]Subrahmanyam K S, Panchakarla L S, Govindaraj A, et al. *J. Phys. Chem. C*, **2009**,**113**(11):4257-4259

[18]Zhang J, Liu X, Blume R, et al. *Science*, **2008**,**322**(5898): 73-77

[19]Liu G, Li X G, Ganesan P, et al. *Electrochim. Acta*, **2010**, **55**(8):2853-2858

[20]Zhao A Q, Masa J, Muhler M, et al. *Electrochim. Acta*, **2013**, **98**:139-145

[21]Ikeda T, Boero M, Huang S F, et al. *J. Phys. Chem. C*, **2008**, **112**(38):14706-14709

[22]Yan N, Chen X. *Nature*, **2015**,**524**(7564):155-157

[23]Wang R F, Wang K, Wang Z H, et al. *J. Power Sources*, **2015**,**297**:295-301

[24]Gao Y J, Chen X, Zhang J G, et al. *ChemPlusChem*, **2015**, **80**(10):1556-1564

[25]Liu X R, Zhang M, Yu D N, et al. *Electrochim. Acta*, **2016**, **215**:223-230

[26]Murthy A P, Theerthagiri J, Premnath K, et al. *J. Phys. Chem. C*, **2017**,**121**(21):11108-11116

[27]Kato M, Murotani T, Yagi I. *Chem. Lett.*, **2016**,**45**(10):1213-1215

[28]Wang J, Zhu H, Chen J D, et al. *Int. J. Hydrogen Energy*, **2016**,41(40):18044-18049

[29]Zhu H, Gu L, Yu D N, et al. *Energy Environ. Sci.*, **2016**,**10**(1):321-330

[30]Liu X, Meng C G, Han Y. *J. Phys. Chem. C*, **2013**,**117**(3):1350-1357

[31]Lu H S, Zhang H M, Liu R R, et al. *Appl. Surf. Sci.*, **2017**, **392**:402-409

[32]Li J X, Zou M Z, Wen W W, et al. *J. Mater. Chem. A*, **2014**, **2**(26):10257-10262

[33]Liu K, Song Y, Chen S W. *Nanoscale*, **2015**,**7**(3):1224-1232

[34]Yuasa M, Oyaizu K, Murata H, et al. *Electrochemistry*, **2012**,**75**(10):800-806